JOURNAL OF MATERIALS SCIENCE 23 (1988) 886–893

# Influences of interfacial bonding strength and scatter of fibre strength on tensile behaviour of unidirectional metal matrix composites

SHOJIRO OCHIAI, KOZO OSAMURA
*Department of Metallurgy, Kyoto University, Sakyo-ku, Kyoto 606, Japan*

The influences of interfacial bonding strength and scatter of strength of fibres on tensile behaviour of unidirectional metal matrix composites, whose matrix has low yield stress in comparison to the strength of fibres, were studied using the Monte-Carlo simulation technique using two-dimensional model composites. The following results were found. The strength of composites increases with increasing bonding strength, especially when the bonding strength exceeds the shear yield stress of the matrix and then remains nearly constant. The strength of composites is very sensitive to bonding strength when the scatter of fibre strength is large, but not when it is small. The fracture mode varies from non-cumulative to cumulative with increasing scatter of fibre strength for both cases of weak and strong interfacial bondings. The fracture surface becomes irregular when bonding strength becomes low and scatter of fibre strength becomes large. The applicability of the Rosen and Zweben models and the rule of mixtures to predict the strength of composites was examined.

## 1. Introduction

It is well known that deformation and fracture behaviour of fibre-reinforced metals is strongly affected by interfacial bonding strength. In the case of weak interfacial bonding, debonding occurs at the interface when the exerted shear stress at the interface exceeds the shear bonding strength of interface. After debonding, only frictional shear stress at the interface contributes to stress transfer from matrix to broken fibres. The frictional shear stress is, however, low in general and therefore the critical length of fibre, which is defined as the necessary length for the fibre to show its full strength, becomes long [1–5]. The increase in critical length due to interfacial debonding causes a reduction in efficiency of reinforcement because the load-bearing capacity of broken fibres decreases in the region from broken ends to half critical length [6, 7]. On the other hand, in the case of strong interfacial bonding, the critical length is short and therefore the efficiency of reinforcement is high, which plays a role in raising the strength of composites, but the stress concentration in the fibres adjacent to broken fibres is high [1–5], and plays a role in reducing the strength of composites.

The influence of interfacial bonding strength on tensile behaviour of composites arises mainly through the factors of stress concentration in the fibres adjacent to broken fibres, and the critical length of the broken fibres. As the breakage of fibres is dependent on scatter or distribution of fibre strength, the scatter of fibre strength has a strong influence on tensile behaviour of composites as well as interfacial bonding strength. It is therefore very important to know the influences of interfacial bonding strength and scatter of fibre strength on mechanical behaviour of composites in a quantitative manner. However, it is very difficult to study such influences experimentally by changing interfacial bonding strength and scatter of fibre strength separately for a given composite system.

This difficulty can be overcome by employing a computer simulation technique in which interfacial bonding strength and scatter of fibre strength can be changed over wide values at will. The aim of the present work is to study the influences of them on tensile behaviour of metal matrix composites by means of this technique, using two-dimensional composites and to obtain fundamental information on this subject. The simulation program employed in the present work has been demonstrated to describe successfully the tensile behaviour of boron–aluminium mono-layer composite specimens [8, 9].

## 2. Experimental procedure

In the present work, the composite was regarded to be composed of tensile stress-carrying fibres and shear stress-carrying matrix. Namely the matrix was regarded to be the medium of stress transfer, giving no contribution to stress of composites, as usually approximated in the shear-lag-analysis [1–5]. This approximation becomes a problem when the volume fraction of fibres, $V_f$, is low and when the yield stress of matrix is high, because the contribution of matrix stress to composite stress cannot be regarded as zero. With this in mind, the $V_f$, average strength of fibres and shear yield stress of matrix, $\tau_y$, were taken to be 0.50, 3 GPa and 50 MPa, respectively, in the present work. Under these conditions, the contribution of matrix stress ($100\,\text{MPa} \times 0.5 = 50\,\text{MPa}$ where 100 MPa is the



0022–2461/88 $03.00 + .12 

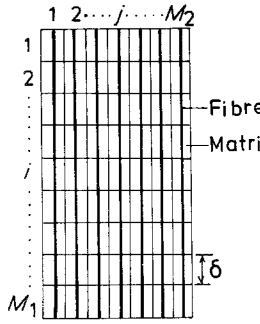


*Figure 1* Schematic representation of the model composite.

tensile yield stress of matrix) is low enough compared with that of fibres (3 GPa × 0.5 = 1.5 GPa in a rough estimation), to allow calculation of the stress concentration factor and critical length by means of the shear-lag-analysis method [1–5].

The configuration of composites used in the present work is schematically shown in Fig. 1. The composites are composed of a number of $M_2$ fibres, each fibre being composed of $M_1$ elements in the longitudinal direction. In the simulation experiments, first the strength of each element was given by the Monte-Carlo method and the tensile behaviour of each element and composite as a whole was investigated by applying strain on the composite step by step. The stress concentration in the fibres adjacent to the broken fibres, and the critical length of the fibres were calculated by the shear-lag-analysis [4, 5]. Details of the procedure of the computer simulation experiments are shown elsewhere [9].

The input values are listed in Table I. Among the input values, interfacial bonding strength in shear $\tau_i$, frictional shear stress at interface after debonding, $\tau_f$, and coefficient of variation of fibre strength, $CV$, were varied while the other values were fixed. The strength of fibres were assumed to obey the Weibull distribution function [10]. The relation of Weibull modulus, $m$, to $CV$ is given by

$$CV = \{\Gamma(1 + 2/m)/[\Gamma(1 + 1/m)]^2 - 1\}^{1/2}$$

where $\Gamma$ is the gamma function. From this relation, for instance, $m$ = 40, 8 and 5 correspond to $CV$ = 3, 15 and 23%, respectively.

The simulation experiments were repeated more than 30 times for a given condition, and average values and standard deviations were obtained.

TABLE I Input values for the present simulation

| | |
|---|---|
| Number of elements in each fibre, $M_1$ | 25 |
| Number of fibres, $M_2$ | 25 |
| Length of composite, $l$ (mm) | 50 |
| Young's modulus of fibre, $E_f$ (GPa) | 400 |
| Shear modulus of matrix, $G_m$ (GPa) | 40 |
| Strain-hardening coefficient of matrix normalized with respect to $G_m$, $\beta$ | 0.01 |
| Shear yield stress of matrix, $\tau_y$ (MPa) | 50 |
| Interfacial bonding strength, $\tau_i$ (MPa) | 25–150 |
| Frictional shear stress after debonding at interface, $\tau_f$ (MPa) | 0 and 5 |
| Diameter of fibre, $d_f$ ($\mu$m) | 100 |
| Volume fraction of fibre, $V_f$ | 0.5 |
| Average strength of fibre $\bar{\sigma}_f^0$ (GPa) | 3 |
| Coefficient of variation of strength of fibre, $CV$ (%) | 0–28 |

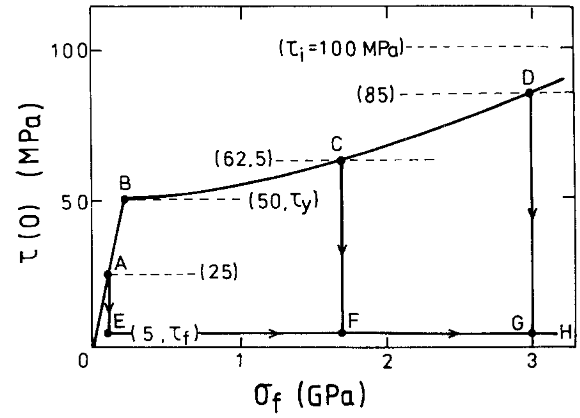


*Figure 2* Variation of $\tau(0)$ as a function of $\sigma_f$. $n$ = 1, $\tau_y$ = 50 MPa, $\tau_f$ = 5 MPa.

## 3. Results and discussion

### 3.1. Relation of interfacial bonding strength to critical length and stress concentration

In this section, the relation of interfacial bonding strength, $\tau_i$, to critical length, $l_c$, and stress concentration in the fibres adjacent to the broken fibres calculated by the shear-lag-analysis [5] using the values of mechanical properties of fibre and matrix shown in Table I, will be shown.

The shear stress between broken and unbroken fibres is highest at the cross-section including the broken end ($x$ = 0) of the broken fibre. This highest shear stress is denoted $\tau(0)$ in this work. Taking the case where one fibre is broken even at low applied stress while other fibres are not broken, $\tau(0)$ increases along 0ABCD as shown in Fig. 2 when interfacial bonding is strong. The regions of 0B and BCD correspond to the regions where the matrix deforms elastically in shear and it deforms plastically in shear, respectively. Here we define the stress of fibre far away from the broken end as $\sigma_f$. If a composite is broken at $\sigma_f$ = 3 GPa, no interfacial debonding occurs as long as $\tau_i$ is higher than 85 MPa, as known from Fig. 2. If $\tau_i$ is lower than 85 MPa, interfacial debonding occurs at the value of $\sigma_f$ corresponding to $\tau(0) = \tau_i$ and the frictional shear stress, $\tau_f$, begins to act at the interface. As a result $\tau(0)$, for instance for $\tau_i$ = 25 and 62.5 MPa, vary along 0AEH and 0BCFH in Fig. 2, respectively. The length of the debonded interface increases rapidly with increasing $\sigma_f$ and, accordingly, the critical aspect ratio $l_c/d_f$, where $d_f$ is the diameter of fibre, also increases as shown in Fig. 3a. On the

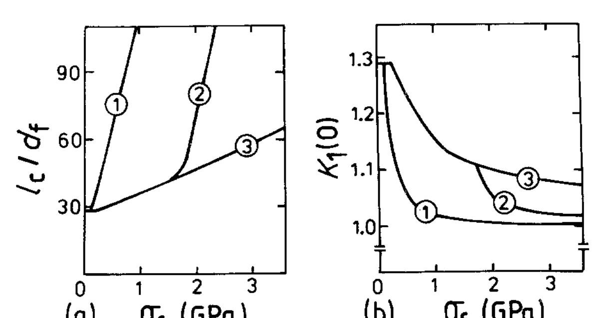


*Figure 3* Variation of $l_c/d_f$ (a) and $K_1(0)$ (b) as a function of $\sigma_f$. (1) $\tau_i$ = 25 MPa, (2) $\tau_i$ = 62.5 MPa, (3) $\tau_i$ = 100 MPa.

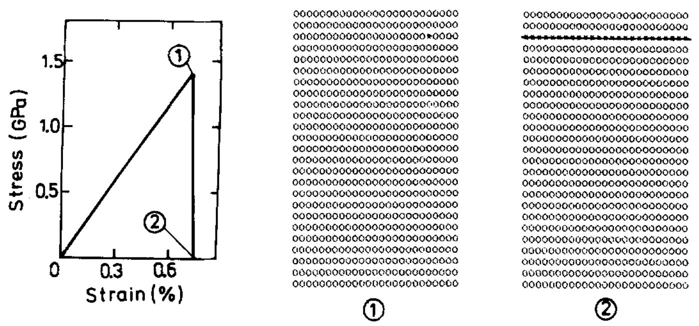


*Figure 4* Typical stress–strain curve of the strongly bonded composite with small $CV$ ($\tau_i = 2\tau_y = 100$ MPa and $CV = 3\%$), together with the fracture morphology of fibres at point 1 and fracture surface of the composite, point 2. $\tau_f = 5$ MPa.

other hand, the stress concentration in the fibres adjacent to the broken fibre decreases with increasing length of debonded interface as shown in Fig. 3b where the $K_I(0)$ is the stress concentration factor at $x = 0$. In this way, the debonding gives two opposite factors: an increase in critical length, which acts to reduce strength of composites, and a decrease in stress concentration factor, which acts to raise it.

## 3.2. Fracture process of fibres in composites

In the present work, the average strength of fibres was taken to be 3 GPa. At $\sigma_f = 3$ GPa, the $l_c/d_f$ is about 50 in the case of strong interface of $\tau_i = 100$ MPa, as shown in Fig. 3. Then the aspect ratio of each element in Fig. 1 was taken to be 25 in the simulation experiment. When interfacial bonding is weak and debonding occurs at the interface, there arises three kinds of elements [9]: broken elements (B elements), ineffective elements (I elements) which are not broken but cannot carry applied load, existing near the broken ends of broken fibres, and stress carrying elements (S elements). In the case of strong interfacial bonding, no I elements arise, but in the case of weak bonding, all these elements are seen. When interfacial bonding is weak and the frictional shear stress after debonding is low, $l_c$ becomes large, leading to an increase in the number of I elements.

The fracture process of fibres in composites depends on the combination of the values of $\tau_i$ and $CV$. Figs 4 to 7 show typical stress–strain curves, and locations of B(*), I(I) and S elements (0) at the given strains shown in the stress–strain curves and fracture morphology of the composites as a whole for the combinations of high $\tau_i$ and small $CV$, low $\tau_i$ and small $CV$, high $\tau_i$ and large $CV$, and low $\tau_i$ and large $CV$, respectively. As already stated, the contribution of matrix stress to composite stress is neglected in the stress–strain curves. In the case of strong interfacial bonding of $\tau_i = 2\tau_y = 100$ MPa, the I element does not appear when one fibre is broken alone, but it appears below and above the B elements when two (or more) successive fibres are broken in a row in one cross-section, as shown in Figs 4 and 6. This results from the tendency for the critical length of broken fibres in a row to increase with increasing number of broken fibres in a row [1–5]. On the other hand, in the case of weak interfacial bonding of $\tau_i = 0.5\tau_y = 25$ MPa, the I elements appear even when one fibre alone is broken, because of long critical length, as shown in Figs 5 and 7.

The features found in Figs 4 to 7 can be summarized as follows. (i) In the combination of high $\tau_i$ and small $CV$, the breakage of a few fibres causes breakages of neighbouring fibres one after another, resulting in non-cumulative fracture mode of composites as a whole. (ii) In the combination of high $\tau_i$ and large $CV$, the breakage of fibres is cumulative. Herring *et al.* [11] have found experimentally the same features of (i) and (ii) in their boron–aluminium composites by changing $CV$. Their results have been successfully simulated by the present simulation program in our former work [9]. (iii) In the combination of low $\tau_i$ and small $CV$, the breakage of a few fibres causes breakage of neighbouring fibres one after another, as well as in the combination of high $\tau_i$ and small $CV$, but the fracture morphology between the two combinations is different in respect of pull-out of fibres found when $\tau_i$ is low but not when $\tau_i$ is high. In the case of both low and high $\tau_i$, when $CV$ is small, the initiation of fracture of composites is common in that the breakage of a few fibres causes breakage of other fibres and composites as a whole. However, the fracture process of composites is different in the two cases. When $\tau_i$ is high, as the strength of each element or fibre for small $CV$ is very little different from each other and the stress concentration in the fibres adjacent to broken fibres is high compared with that for low $\tau_i$, the unbroken fibres are broken one after another, resulting in the flat fracture surface just perpendicular to the tensile axis. On the other hand, when $\tau_i$ is low, the I elements appear after

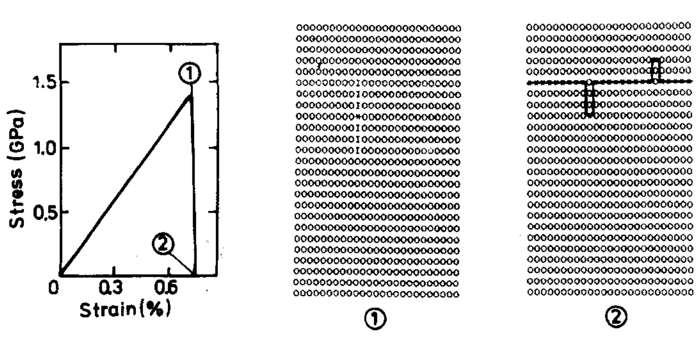


*Figure 5* Typical stress–strain curve of the weakly bonded composite with small $CV$ ($\tau_i = 0.5\tau_y = 25$ MPa and $CV = 3\%$), together with the fracture morphology at point 1 and fracture surface of composite, point 2. $\tau_f = 5$ MPa.

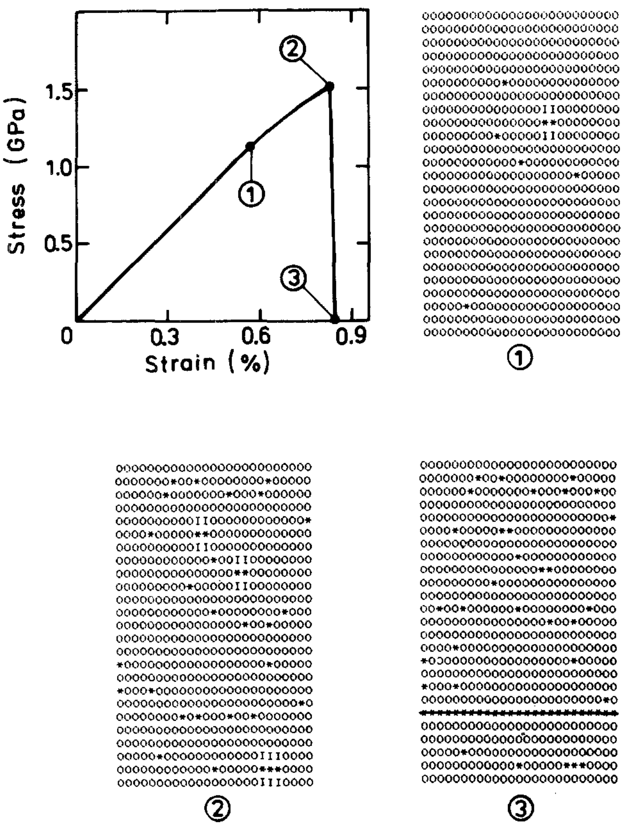


*Figure 6* Typical stress–strain curve of the strongly bonded composite with large $CV$ ($\tau_i = 2\tau_y = 100$ MPa and $CV = 23\%$), together with the fracture morphology of fibres at points 1 and 2, and fracture surface of composite, point 3. $\tau_f = 5$ MPa.

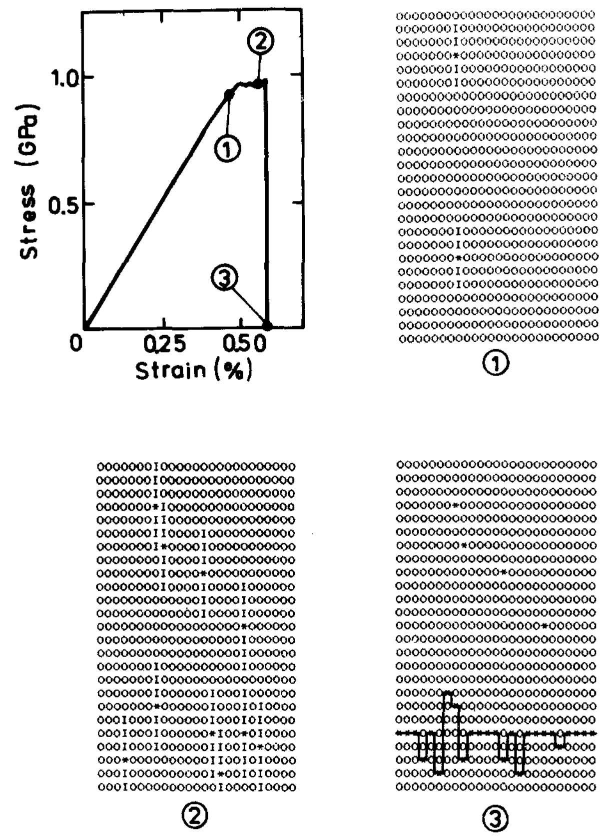


*Figure 7* Typical stress–strain curve of the weakly bonded composite with large $CV$ ($\tau_i = 0.5\tau_y = 25$ MPa and $CV = 23\%$), together with the fracture morphology of fibres at points 1 and 2, and fracture surface of composite, point 3. $\tau_f = 5$ MPa.

breakage of the fibres. Therefore when $\tau_i$ is low, the S elements in the cross-section containing B and I elements should carry a higher load than those in the cross-section containing no B and I elements to maintain the applied load which should be equal in any cross-section. Considering the situation where only one element is broken and there exist one B element and more than two I elements below and above the B element, if the S elements in the cross-sections containing I elements are weaker than those in the cross-sections containing the B element, the S elements in the former cross-sections could be broken before those in the latter cross-section. Namely when $CV$ is small, in the case of high $\tau_i$, the fracture of composites occurs in the cross-section containing B element, but in the case of low $\tau_i$, it occurs not only in the cross-section containing the B element but also in the cross-sections containing I elements. As the number of I elements becomes larger than that of B elements when $\tau_i$ is low, the fracture surface of weakly bonded composites becomes irregular, accompanied by pull-out. (iv) In the combination of low $\tau_i$ and large $CV$, the breakage of fibres occurs cumulatively and the fracture surface of composites is very irregular.

In the stress–strain curves shown in Figs 4 to 7, the stress of composites drops suddenly at fracture, indicating that the fracture of composites occurs catastrophically in the above combinations of $\tau_i$ and $CV$. However, this is not a general feature when $\tau_i$ is low. In the above combinations, the frictional shear stress, $\tau_f$, after debonding was taken to be 5 MPa. When $\tau_f$ was taken to be smaller than this value, the fracture of composites became rather non-catastrophic. Fig. 8 shows an example of $\tau_i = 25$ MPa and $\tau_f = 0$ MPa, corresponding to the case where the critical length is longer than the length of composites and any elements in broken fibres cannot carry an applied load, because the elements below and above the B element become I elements, and $K_1(0)$ is nearly equal to unity. In this example, breakage of fibres occurs in the order of weakness and no catastrophic fracture of composites as a whole occurs. In this way, the final fracture behaviour of composites as a whole is dependent on $\tau_i$ and $\tau_f$, which determines critical length and stress concentration. When the critical length becomes very long and accordingly the stress concentration becomes very low, composites begin to show the non-catastrophic fracture mode.

As stated above, the breakage of fibres occurs cumulatively when $CV$ is large but non-cumulatively when $CV$ is small. The values of $\tau_i$ and $\tau_f$ affect the number of I elements for one B element. Fig. 9 shows an example of the number of B elements, $N^*$, and the total number of B and I elements ($N^{\mathrm{I}}$), $N^* + N^{\mathrm{I}}$, which cannot carry applied load, plotted against strain applied to the composites. In this example, only the cases of $CV = 12$ and $28\%$, where breakage of fibres occurs cumulatively, are presented. Not only in these cases but also in other cases including the cases where breakage of fibres occurs non-cumulatively, is $N^* + N^{\mathrm{I}}$ larger than $N^*$ in the case of weak interfacial bonding, while $N^* + N^{\mathrm{I}}$ is very little different from $N^*$ in the case of strong interfacial bonding.

Here a simple concept used in the present simulation

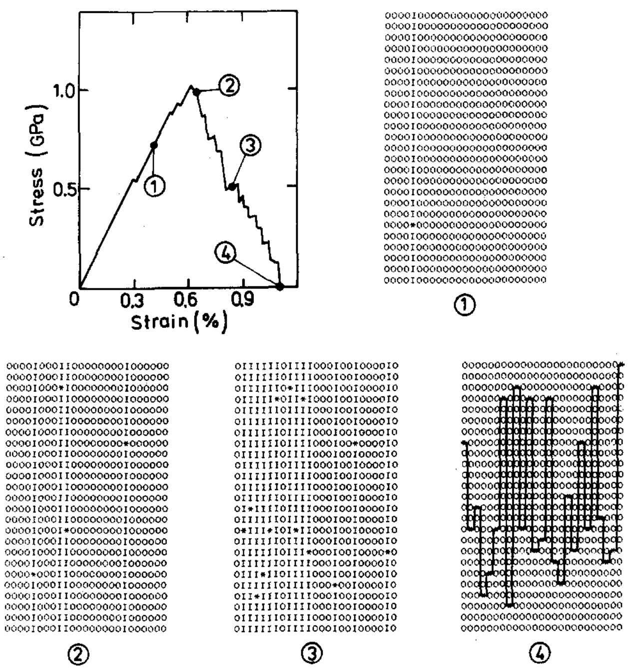

*Figure 8* Typical stress–strain curve of the composite with low values of $\tau_i$ (25 MPa) and $\tau_f$ (0 MPa), together with the fracture morphology of fibres at points 1 to 3 and fracture surface of composite, point 4. $CV$ = 23%.

experiment is briefly stated in order to show how the efficiency of reinforcement is affected by the critical length. When there is no breakage of fibres and all elements carry applied load, the load carried by composites is given by $\varepsilon E_f A_f M_2$ where $\varepsilon$ is the strain of composites, $E_f$ is the Young's modulus of fibres and $M_2$ is the number of fibres. This load is denoted $L_{c,0}$. In this situation, the stress of all elements is $\varepsilon E_f$. When some elements are broken, $\varepsilon$ is approximately given by $(\Sigma_{i=1}^{M_1} \varepsilon_i)/M_1$ where $\varepsilon_i$ is the average strain of the S elements in the $i$th cross-section in Fig. 1. The load borne by the $i$th cross-section, $L_c$, is given by $A_f \varepsilon_i E_f (M_2 - n_i')$ where $n_i'$ is the total number of B and I elements in the $i$th cross-section. As $L_c$ should be equal in any cross-section, it is given by

$$L_c = A_f \varepsilon E_f M_1 \Big/ \left[ \sum_{i=1}^{M_1} (M_2 - n_i')^{-1} \right]$$

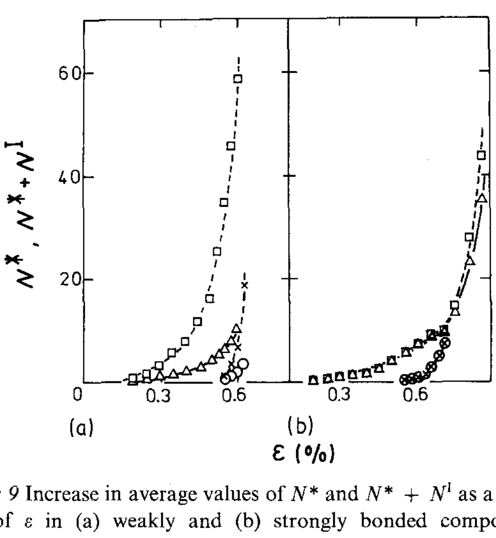

*Figure 9* Increase in average values of $N^*$ and $N^* + N^I$ as a function of $\varepsilon$ in (a) weakly and (b) strongly bonded composites. $\beta = 0.01$, $\tau_f = 5$ MPa, $\tau_i = 25$ MPa. (○) $N^*$ ($CV$ = 12%), (×) $N^* + N^I$ ($CV$ = 12%), (△) $N^*$ ($CV$ = 28%), (□) $N^* + N^I$ ($CV$ = 28%).

by combining the above relations. Defining the efficiency of reinforcement as the ratio of $L_c$, which composites in fact carry, to $L_{c,0}$, which composites could carry if it were not for breakage of fibres, the efficiency is given by

$$L_c/L_{c,0} = (M_1/M_2) \Big/ \left[ \sum_{i=1}^{M_1} (M_2 - n_i')^{-1} \right]$$

When there is no breakage of fibres, the efficiency is unity. The critical length affects the efficiency by changing $n_i'$. This procedure to derive $L_c/L_{c,0}$ is not rigid in that the stress concentration in the S elements is not incorporated. This can, however, be applied to a first approximation when the stress concentration factor is nearly unity. In this work, the stress concentration factor at high $\sigma_f$ was very little different from unity especially when interfacial bonding is weak, as typically shown in Fig. 3b, which allows this procedure to be applied for weakly bonded composites. For strongly bonded composites, this is not adequate, but, as $\tau_y$ is taken to be low in this work, the stress concentration factor is not high at high $\sigma_f$, as shown in Fig. 3b, it can be applied to a first approximation with a loss of accuracy.

Fig. 10 shows some examples of the location and number of I elements under a given number of B elements of 8 for strong (a), weak (b) and extremely weak (c) interfacial bondings were $\tau_f$ was taken to be 5 MPa. The efficiency for (a) to (c) were calculated to be 0.98, 0.89 and 0.68, respectively. It is evident that the lower the interfacial bonding strength, the lower the efficiency becomes. As shown in Fig. 9, as $N^* + N^I$ is large when $CV$ is large, $n_i'$ also becomes large, leading to low efficiency of reinforcement especially when interfacial bonding is weak.

### 3.3. Strength of composites

Fig. 11 shows the relation of strength of composites, $\sigma_c$, to $\tau_i$ for $CV$ = 23, 15 and 3%. The following features are found. (a) When $CV$ is very small, $\sigma_c$ remains nearly constant, being independent of $\tau_i$, but when $CV$ is large, $\sigma_c$ increases with increasing $\tau_i$. When $CV$ is very small, as the breakage of a few fibres causes breakage of remaining fibres which have nearly the same strength as the broken fibres, as already stated, $\sigma_c$ is merely dependent on $\tau_i$. (b) Except for the cases of very small $CV$, $\sigma_c$ increases slightly with increasing $\tau_i$ for $\tau_i \leqq \tau_y = 50$ MPa but it increases rapidly for $\tau_i \geqq \tau_y$ and then it remains nearly constant at high $\tau_i$. This variation of $\sigma_c$ corresponds to the variation of critical length at a given $\sigma_f$, which decreases slightly with increasing $\tau_i$ for $\tau_i \leqq \tau_y$, but decreases rapidly for $\tau_i \geqq \tau_y$ and remains nearly constant at high $\tau_i$ where the critical length is determined not by interfacial bonding strength but by the shear stress of the matrix [5]. The stress concentration in the fibres adjacent to broken fibres at a given $\sigma_f$ increases with increasing $\tau_i$ [5], which acts to reduce $\sigma_c$ with increasing $\tau_i$. However, within the range of the present work, the decrease in critical length with increasing $\tau_i$, which acts to raise $\sigma_c$, contributes to an increase in $\sigma_c$ despite the detrimental effect due to increase in stress concentration. However, this might not be a general feature

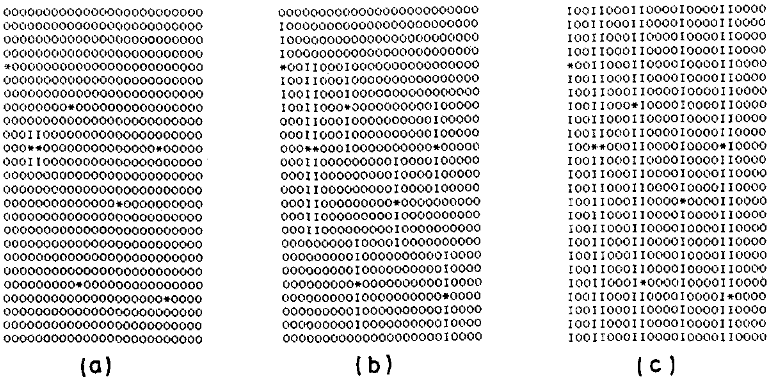


*Figure 10* Examples of distribution of B("*"), I("I") and S("0") elements for (a) strong, (b) weak and (c) extremely weak interfacial bonding strengths.

of metal matrix composites. In this work, the $\tau_y$ is taken to be low, which leads to a low stress concentration factor at high $\sigma_f$ even for high $\tau_i$ as shown in Fig. 3b. In such a case, the change in critical length with increasing $\tau_i$ is more effective than that in stress concentration, which is not high even for high $\tau_i$. On the other hand, if $\tau_y$ is very high, the stress concentration becomes high for a given $\sigma_f$ when interfacial bonding is strong [4, 5]. The high stress concentration could reduce $\sigma_c$ in spite of the decrease in critical length. Namely, too strong an interface might cause reduction in $\sigma_c$ when $\tau_y$ is very high. On this point, further study is needed.

Fig. 12 shows the variation of $\sigma_c$ with increasing $CV$ for $\tau_i = 2\tau_y$, $1.5\tau_y$ and $0.5\tau_y$ under a given value of $\tau_f = 5$ MPa, together with the relation of $\sigma_c$ to $CV$ for $\tau_i = 0.5\tau_y$ and $\tau_f = 0$ MPa for comparison. The larger the $CV$, the larger the difference in $\sigma_c$ between strong (○) and weak (△) interfacial bondings becomes. Namely, the larger the $CV$, the more sensitive $\sigma_c$ becomes $\tau_i$. This tendency is accounted for as follows. When interfacial bonding is weak, the number of I elements increases, which reduces the efficiency of reinforcement. Especially when $CV$ is large, as the breakage of fibres occurs cumulatively and therefore the number of B elements is large, the number of I elements becomes very large if $\tau_i$ is low, leading to low efficiency of reinforcement, resulting in low $\sigma_c$. On the other hand, when interfacial bonding is strong, the fracture of composites tends to occur in one cross-section without pull-out of fibres, because the pull-out is not allowed due to short critical length. In order to break elements in one cross-section, high stress is required when $CV$ is large as long as the fibre strength obeys the Weibull distribution function, because the Weibull distribution function supplies the feature that the larger the $CV$, the higher the strength of elements becomes. For instance, the average strengths of elements are $3.25 \pm 0.10$, $4.49 \pm 0.67$ and $5.71 \pm 1.31$ GPa for $CV = 3$, 15 and 23%, respectively, while the average strengths of fibres are $3 \pm 0.09$, $3 \pm 0.45$ and $3 \pm 0.69$, respectively, in the present work. Thus the larger $CV$, the higher $\sigma_c$ becomes at high $\tau_i$, while the larger $CV$, the lower $\sigma_c$ becomes at low $\tau_i$, as stated above. This is the reason why $\sigma_c$ is sensitive to $\tau_i$ when $CV$ is large. On the other hand, when $CV$ is small, the difference in strength of fibres (and also elements) is small and the breakage of a few fibres causes fracture of composites for both cases of strong and weak interfacial bondings. This leads to $\sigma_c$ for small $CV$ not being sensitive to $\tau_i$.

It is very interesting in Fig. 12 that $\sigma_c$ decreases with increasing $CV$, reaching the lowest value at about 5% $CV$ and then increasing when $\tau_i$ is high, while $\sigma_c$ decreases monotonically with increasing $CV$ when $\tau_i$ is low. When $\tau_i$ is low, the number of both of B and I

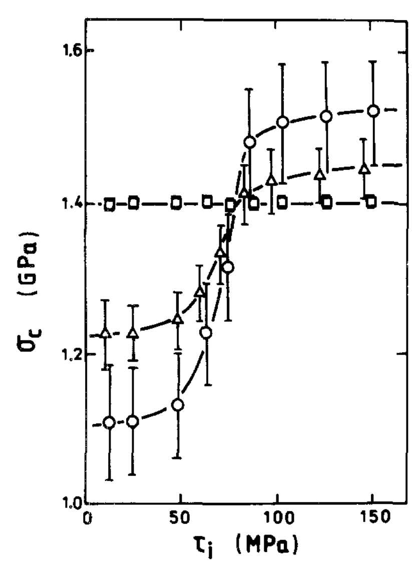


*Figure 11* Variation of $\sigma_c$ as a function of $\tau_i$ for $CV =$ (○) 23, (△) 15 and (□) 3%. $\beta = 0.01$, $\tau_f = 5$ MPa, $\tau_y = 50$ MPa.

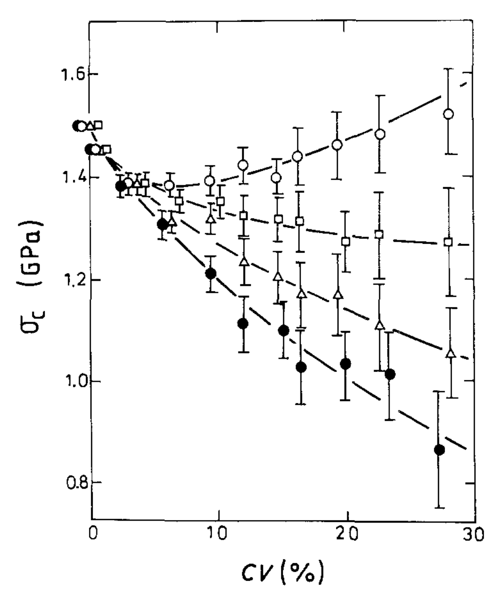


*Figure 12* Variation of $\sigma_c$ as a function of $CV$. $\tau_y = 50$ MPa, $\beta = 0.01$. (○) $\tau_i = 100$ MPa, $\tau_f = 5$ MPa; (□) $\tau_i = 75$ MPa, $\tau_f = 5$ MPa; (△) $\tau_i = 25$ MPa, $\tau_f = 5$ MPa; (●) $\tau_i = 25$ MPa, $\tau_f = 0$ MPa.

elements increases with increasing $CV$, leading to a reduction in $\sigma_c$ with increasing $CV$. The variation of $\sigma_c$ as a function of $CV$ for high $\tau_i$ is explained as follows. In the range of small $CV$, the breakage of weaker fibres causes fracture of composites. The strength of weaker fibres becomes low with increasing $CV$ because the scatter of fibre strength increases with increasing $CV$. Thus $\sigma_c$ becomes low with increasing $CV$ as long as the composites show a non-cumulative fracture mode. However, the fracture of fibres occurs cumulatively when $CV$ becomes large. In the range of $CV$ where the cumulative fracture mode occurs, the average strength of elements increases with increasing $CV$, as stated above, leading to an increase in $\sigma_c$ with increasing $CV$.

In the case where the interfacial bonding strength is intermediate, $\sigma_c$ shows intermediate values between the values of $\sigma_c$ for strong and weak interfaces, as shown in Fig. 12.

As stated above, $\tau_f$ also has an affect on $\sigma_c$ when $\tau_i$ is low. In this condition, the critical length at fracture of the composites is far longer than the gauge length of the composites and also the stress concentration is nearly unity. Therefore each fibre is broken, depending on its strength. Such a fracture behaviour is the same as that of fibre-bundles without matrix.

### 3.4. Prediction of strength of composites based on the Rosen and Zweben models, and the rule of mixtures

Several simple models have been presented to predict strength of composites: Rosen model [12, 13], Zweben model [14, 15] and the rule of mixtures [6, 16]. If these models can be utilized, it is very convenient because they require only simple calculation. These models have following features.

The Rosen model (R model) treats the case where the fibres are broken cumulatively. In this and Zweben's models, the fibres in composites are regarded to be composed of a number of $N$ links with a length $l_c$ where $N$ is given by $l/l_c$ ($l$ = length of composites). $\sigma_c$ is given by the bundle strength of the fibres,

$$\sigma_c = \sigma_0 V_f (l_c m e)^{-1/m}$$

where $\sigma_0$ and $m$ are the Weibull constants and $e$ is the base of natural logarithm. In this model, the stress concentration arising from broken fibres is ignored. Therefore, this can be applied only to the case where the stress concentration is nearly unity. Such a case may correspond to the case where $\tau_i$ and $\tau_f$ are low.

The Zweben model treats the case of non-cumulative fracture mode. In this model, the stress concentration plays a dominant role in contrast to that in the R model. The difficulty of application of this model is that the correspondence of the number of breakages of fibres to fracture of composites as a whole should be known beforehand. In the case of boron–aluminium composites, Zweben and Rosen [14, 15] have found that the fracture of composites occurs when "at least more than two successive links" are broken. The expected number of "more than two successive broken links" under the fibre stress level of $\sigma_f$, $E_2(\sigma_f)$, for two-dimensional composites, is given by

$$E_2(\sigma_f) = E_1(\sigma_f)\{2[F(K_1\sigma_f) - F(\sigma_f)] - [F(K_1\sigma_f) - F(\sigma_f)]^2\}$$

where $F(\sigma_f)$ is the cumulative distribution function of links with a length $l_c$, $E_1(\sigma_f)$ is the expected number of isolated broken links and $K_1$ is the stress concentration factor. $E_1(\sigma_f)$ is given by

$$E_1(\sigma_f) = M_2 N F(\sigma_f)$$

In the criterion that composites fracture when "more than two successive broken links" appears, $\sigma_c$ is given by $\sigma_f V_f$ where $\sigma_f$ satisfies $E_2(\sigma_f) = 1$. This criterion is, however, not a general one. For instance, Herring *et al.* [11] have found experimentally that only one breakage of fibre causes fracture of boron–aluminium composites as a whole, when $CV$ is small. In such a case, the criterion of fracture of composites should be $E_1(\sigma_f) = 1$. In the present work, the model using the criterion of $E_2(\sigma_f) = 1$ is termed the $E_2$ model and that using $E_1(\sigma_f) = 1$ the $E_1$ model.

The rule of mixtures [6, 16] is a well known approximation, according to which $\sigma_c$ is given by

$$\sigma_c = \sigma_{fu}^0 V_f$$

where $\sigma_{fu}^0$ is the average strength of fibres. In this model, the influence of interfacial bonding and scatter of fibre strength on strength of composites are neglected.

To date, each model has been found to describe well the strength of composites in some composites but not in others. As there is no systematic investigation on the applicability of these models to date, the conditions under which each model can describe $\sigma_c$, will be examined.

Figs 13 and 14 show a comparison of the values of $\sigma_c$ predicted by the R, $E_1$, $E_2$ and ROM models with those obtained by the present simulation experiments. The following features can be seen in Figs 13 and 14. (1) When $CV$ is small (about less than 5%), $\sigma_c$ predicted by the $E_1$ model agrees well with that obtained by the simulation experiments for both cases of strong and

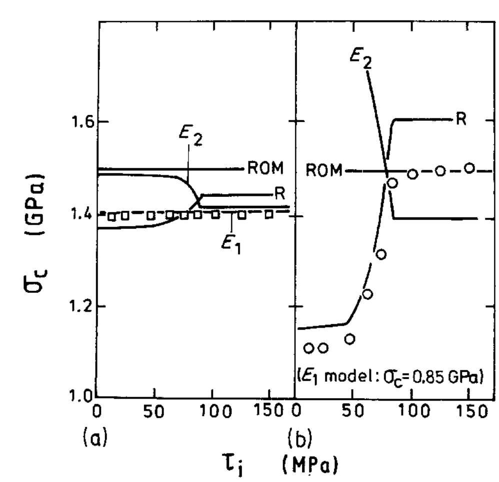


*Figure 13* Relation of $\sigma_c$ to $\tau_i$ predicted by the R, $E_1$, $E_2$ and ROM models, together with the experimental relation for comparison. The $E_1$ model gives $\sigma_c = 0.85$ GPa for $CV = 23\%$, which is independent of $\tau_i$. This value is too low to be drawn in (b). $\tau_y = 50$ MPa, $\beta = 0.01$. (a) $CV = 3\%$. (b) $CV = 23\%$.

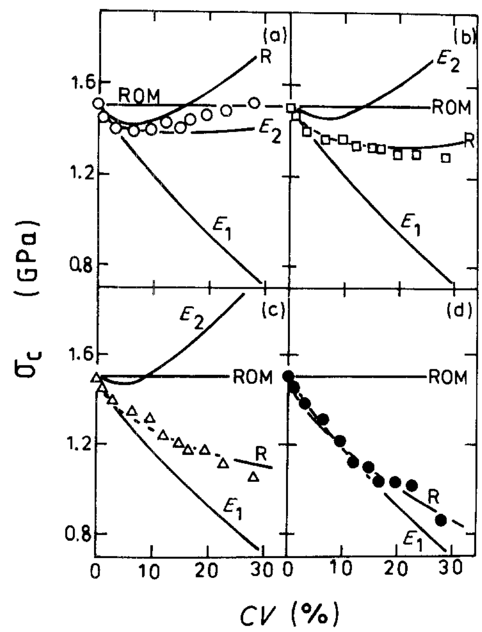


*Figure 14* Relation of $\sigma_c$ to $CV$ predicted by the R, $E_1$, $E_2$ and ROM models, together with the experimental relation for comparison. The $\sigma_c$ for $\tau_i$ = 25 MPa and $\tau_f$ = 0 MPa in (d) cannot be calculated based on the $E_2$ model because $K_1$ = 1. $\tau_y$ = 50 MPa, $\beta$ = 0.01. (a) $\tau_i$ = 100 MPa, $\tau_f$ = 5 MPa. (b) $\tau_i$ = 75 MPa, $\tau_f$ = 5 MPa. (c) $\tau_i$ = 25 MPa, $\tau_f$ = 5 MPa. (d) $\tau_i$ = 25 MPa, $\tau_f$ = 0 MPa.

weak interfaces. (2) In the range where the $CV$ is larger than about 5% but smaller than about 15%, when interfacial bonding is strong, the values of $\sigma_c$ predicted by the $E_2$ model are nearly the same as the experimental values, while the R and ROM models give a little and much higher values than the experimental values, respectively. The value of $CV$ in Zweben's boron–aluminium composites whose $\sigma_c$ could be described by the $E_2$ model is within this range of $CV$ [15]. When interfacial bonding is weak ($\tau_i$ = 75 and 25 MPa), $\sigma_c$ predicted by the R model agrees fairly well with the experimental one. (3) In the range where the $CV$ is larger than about 15%, when interfacial bonding is strong, the experimental values exist within the values predicted by the R and $E_2$ model, and they agree with those predicted by the ROM. However, it should be noted that the tendency for $\sigma_c$ to increase with increasing $CV$ can be predicted by the R and $E_2$ models but not by the ROM. In the case of weak interfacial bonding, $\sigma_c$ predicted by the R model agrees fairly well with the experimental one.

In this work, $\tau_y$ was taken to be low in comparison to the strength of fibres, and fundamental information for low $\tau_y$ has been obtained. However, in future, high-strength alloys will be employed as matrix materials. For such a case, the present simulation method should be modified in order to simulate the behaviour.

## 4. Conclusions

The tensile behaviour of metal matrix composites, whose matrix has a relatively low yield stress in comparison with the strength of fibres, has been studied by means of the computer simulation technique using a two-dimensional model. The main results are as follows.

1. In the range where the interfacial bonding strength in shear is lower than the shear yield stress of the matrix, the strength of composites increases slightly with increasing interfacial bonding strength, and in the range where the bonding strength is higher than the shear yield stress of the matrix, it increases rapidly with increasing bonding strength. However, in the range where the bonding strength is high enough to suppress debonding at interface, it remains nearly constant, being independent of the bonding strength.
2. The larger the scatter of fibre strength, the more sensitive to interfacial bonding strength the strength of composites becomes.
3. When the scatter of fibre strength is small, breakage of a few fibres causes fracture of composites as a whole, resulting in a non-cumulative fracture mode, while, when the scatter is large, the fracture of fibres occurs cumulatively in the case of both strong and weak interfaces.
4. The irregularities of the fracture surface of the composites due to pull-out of fibres are dependent on both interfacial bonding strength and scatter of fibre strength. The weaker the interfacial bonding and the larger the scatter of fibre strength, the more irregular the fracture surface becomes.
5. It was shown how the Rosen and Zweben models and the rule of mixtures can or cannot predict the strength of composites in various conditions of interfacial bonding strength and scatter of fibre strength.


## Acknowledgement

The authors wish to thank Light Metals Education Foundation Inc., Osaka, Japan, for financial support.


## References


1. J. M. HEDGEPETH, NASA TN D-882 (1961).
2. W. B. FICHTER, NASA TN D-5453 (1969).
3. C. ZWEBEN, *Eng. Fract. Mech.* **6** (1974) 1.
4. S. OCHIAI, K. ABE and K. OSAMURA, *J. Jpn Inst. Metals* **48** (1984) 1021.
5. *Idem*, *Z. Metallkde* **76** (1985) 299.
6. A. KELLY and W. R. TYSON, *J. Mech. Phys. Solids* **13** (1965) 329.
7. A. KELLY, in "Strong Solids" (Oxford University Press, Oxford, 1966), translated into Japanese by Y. Murakami, "Fukugo-Zairyo" (Maruzen, Tokyo, 1971) p. 136.
8. S. OCHIAI, K. ABE and K. OSAMURA, *J. Jpn Inst. Metals* **48** (1984) 1028.
9. S. OCHIAI, K. OSAMURA and K. ABE, *Z. Metallkde* **76** (1985) 402.
10. W. WEIBULL, *J. Appl. Mech.* **18** (1951) 293.
11. H. W. HERRING, J. L. LYTTON and J. H. STEELE Jr, *Met. Trans.* **4** (1973) 807.
12. B. W. ROSEN, *AIAA J.* **2** (1964) 1985.
13. *Idem*, in "Fiber Composite Materials" (ASM, Metals Park, Ohio, 1965) p. 37.
14. C. ZWEBEN, *AIAA J.* **4** (1968) 2325.
15. C. ZWEBEN and B. W. ROSEN, *J. Mech. Phys. Solids* **18** (1970) 189.
16. D. L. DCDANELS, R. W. JECH and J. W. WEETON, *Trans. Met. Soc. AIME* **233** (1965) 636.



*Received 26 March and accepted 8 June 1987*